Materials Science & Engineering C 90 (2018) 168–179

Contents lists available at ScienceDirect

Materials Science & Engineering C

journal homepage: www.elsevier.com/locate/msec

Intracellular calcium ions and morphological changes of cardiac myoblasts response to an intelligent biodegradable conducting copolymer

Yu Wang[a,1], Wei Zhang[b,1], Lihong Huang[a], Yoshihiro Ito[c], Zongliang Wang[a], Xincui Shi[a], Yen Wei[d], Xiabin Jing[a], Peibiao Zhang[a,*]

[a] Key Laboratory of Polymer Ecomaterials, Changchun Institute of Applied Chemistry, Chinese Academy of Sciences, Changchun 130022, China
[b] School of Life Sciences, Northeast Normal University, Changchun 130022, China
[c] Nano Medical Engineering Laboratory, RIKEN Advanced Science Institute, 2-1 Hirosawa, Wako-shi Saitama, 351-0198, Japan
[d] Department of Chemistry, Tsinghua University, Beijing 100084, China

ARTICLE INFO

Keywords:
Aniline pentamer
Poly(L-lactide)
Biocompatibility
H9c2 cell
Electrical stimulation
Cardiac tissue engineering

ABSTRACT

A novel biodegradable conducting polymer, PLA-b-AP-b-PLA (PAP) triblock copolymer of poly (L-lactide) (PLA) and aniline pentamer (AP) with electroactivity and biodegradability, was synthesized and its potential application in cardiac tissue engineering was studied. The PAP copolymer presented better biocompatibility compared to PANi and PLA because of promoted cell adhesion and spreading of rat cardiac myoblasts (H9c2 cell line) on PAP/PLA thin film. After pulse electrical stimulation (5 V, 1 Hz, 500 ms) for 6 days, the proliferation ratio, and intracellular calcium concentration of H9c2 cells on PAP/PLA were improved significantly. Meanwhile, cell morphology changed by varying the pulse electrical signals. Especially, the oriented pseudopodia-like structure was observed from H9c2 cells on PAP/PLA after electrical stimulation. It is regarded that the novel conducting copolymer could enhance electronic signals transferring between cells because of its special electrochemical properties, which may result in the differentiation of cardiac myoblasts.

1. Introduction

Heart failure is a major cause of death in recent years because of the inability of myocardium regeneration after injury [1,2]. The traditional treatments include organ transplantation, surgical reconstruction, mechanical or synthetic devices. Tissue engineering is a new and promising therapy for patients with heart failure [3,4]. The biomaterials, including collagen, poly (glycolic acid) (PGA) and PLA play an important role in construction of engineered heart tissue [5]. The problems related to myocardial tissue engineering are materials lack of response to environment and the interaction of electrophysiology among cells in engineered heart tissue [6–8].

Electrically conductive polymers have been discovered and explored for increasing applications in many areas of applied chemistry and physics for many years, such as light emitting diodes (LEDs), electrochromic materials, anti-static coatings, solar cells, batteries, chemical sensors, and anti-corrosion coatings [9]. The award of the Nobel Prize in Chemistry in 2000 to H. Shirakawa, A. MacDiarmid and A. Heeger for their pioneering work on conducting polymers widely recognized the importance of these materials and has prompted even more vigorous research in the field [10]. More recently, there is a growing interest in conductive polymers also for various biomedical applications [11,12], including biosensors [13–15], drug delivery [16,17], and tissue engineering [18–20]. The most widely investigated conducting polymers include polypyrrole (PPy), polyaniline (PANi), poly (phenylenevinylene), and polythiophene. PPy is one of the first conducting polymers studied for its effect on mammalian cells [12]. PPy doped with *p*-toluene sulphonate (pTS) and neurotrophin-3 with electrical stimulation of a biphasic current pulse has been reported to significantly improve neurite outgrowth from the explants [21]. There is minimal tissue response to implanted PPy and some evidence of cytotoxicity after long time exposure to current (e.g., 96 h exposure to 1 mA) [22,23]. PANi is another conducting polymer explored for tissue engineering applications, which has been suggested that perhaps the compatibility of PANi is specific to particular cells [12]. Thin layers of fibrous tissue encapsulating unmodified PANi implants and immune response cells (i.e., mast cells) have been observed in an in vivo study [24]. Therefore, although conductive polymers exhibit an attractive

* Corresponding author at: Key Laboratory of Polymer Ecomaterials, Changchun Institute of Applied Chemistry, Chinese Academy of Sciences, Renmin Street No. 5625, Changchun TX:130022, China.
E-mail address: zhangpb@ciac.ac.cn (P. Zhang).
[1] These authors contributed equally to this work.

https://doi.org/10.1016/j.msec.2018.04.061
Received 22 August 2017; Received in revised form 29 March 2018; Accepted 19 April 2018
Available online 22 April 2018
0928-4931/

prospect in improving many cell functions, such as cell attachment, proliferation, migration, and differentiation through electrical stimulation, the biocompatibility of conductive polymers is still a critical limitation in application of tissue engineering.

To improve its biocompatibility, PANi has been blended or grafted with collagen [25], gelatin [18], starch [26], chitosan [27,28], poly(L-lactide-*co*-epsilon-caprolactone (PLCL) [29] and poly(lactic acid) (PLA) [30,31]. Higher adhesion of human dermal fibroblasts, NIH-3T3 fibroblasts and C_2C_{12} myoblasts has been observed on nanofiber substrates of blended polyaniline and PLCL [29]. Porcine skeletal muscle cells could grow as well on the composite films of polyaniline nanofibers and collagen as on collagen [25]. Meanwhile, the growth of NIH-3T3 fibroblasts on blended PANi materials is enhanced under the stimulation of various direct current flows [29].

With the increasing interests in cardiac tissue engineering application of conducting polymers, rat cardiac myoblasts (H9c2 cell line) have been used to culture on PANi or PANi-gelatin blend materials [18,32]. In the study of cardiac tissue engineering, various materials have been applied in culture or construction of artificial myocardial tissue grafts [33,34]. Electrical communication between cardiomyocytes is necessary for native heart tissue or even for functional artificial cardiac tissue [34]. Chemical or electrical stimulation have been used in inducing cardiac progenitor cells progress to organized contracting myocytes [35]. These specific demands lead the researchers to search for biocompatible conducting or electroactive polymers which are expected to control the shape and function of anchorage-dependent cardiomyocytes with electrical currents through their electroactive surfaces. Both the non-conductive emeraldine base (PANi) and its conductive salt (E-PANi) forms of polyaniline have been found to be biocompatible, viz., allowing for cell attachment and proliferation [32]. But the initial adhesion of H9c2 cells to both PANi and E-PANi is slightly reduced. To improve its biocompatibility, the PANi-gelatin blend fibers have been fabricated and the attachment and proliferation of H9c2 cells on these fibers are enhanced greatly [18]. These results demonstrate the potential application of PANi as an electroactive polymer in cardiac tissue engineering. However, the lack of biodegradability of PANi is another outstanding problem related to the applications of electroactive polymers as tissue engineering scaffolds.

To solve the problem, a PLA-b-AP-b-PLA (PAP) triblock copolymer with good electroactivity and biodegradability was designed and synthesized in our group by coupling an electroactive carboxyl-capped AP with two biodegradable bihydroxyl-capped PLAs via a condensation reaction [36]. The PAP copolymer exhibited excellent electroactivity similar to the AP and PANi. The electrical conductivity of the PAP copolymer film ($\sim 5 \times 10^6$ S/cm) was in the semiconductor region. In vitro degradation test shows that the copolymer is capable of degradability and the degradation product AP with the molecular weight of 672.5 is expected to be consumed by macrophages during the normal tissue restoration [12,16]. It will reduce chances of long term adverse responses. In the biomedical application, PAP copolymer should be non-toxic and suitable for cell adhesion and growth of Rat C6 glioma cells [12]. A similar block copolymer of aniline pentamer and polyglycolide (PGA) is reported by Ding et al. and shows good biodegradability [37]. In in vitro degradation test of total 4 months, the copolymer degraded rapidly in the first 30 days because of the cleavage of the ester bond in the backbone, then slowly in the following 60 days, and no further degradation was observed in the last 30 days.

The aim of this work was to investigate the possible application of biodegradable PAP conducting copolymer in cardiac tissue engineering through morphological observation and intracellular calcium analysis of cardiac myoblasts. Cell adhesion and spreading of H9c2 cell line on the thin films of PAP blended PLA (PAP/PLA, w/w = 1:1) were investigated. The effects of pulse electrical stimulation on cell growth, morphology changes and intracellular calcium content of H9c2 on the surfaces of PAP/PLA were subsequently assessed by cell culture and Ca^{2+} imaging.

2. Materials and methods

2.1. Materials

L-Lactide (LLA) was purchased from Purac, Holland. *N*-methyl-pyrrolidone (NMP) and toluene were distilled after drying with CaH_2. 1,4-Butanediol (BDO), stannous octoate [$Sn(Oct)_2$, 95%], *p*-phenylenediamine, *N*-phenyl-1,4-phenylenediamine, *N*,*N*′-dicyclohexyl carbodiimide (DCC), 4-dimethylaminopyridine (DMAP), butane diacid anhydride, camphorsulfonic acid (CSA) and ammonium persulfate were purchased from Aldrich and were used as received without further purification. *N*,*N*-dimethylformamide (DMF), tetrahydrofuran (THF), methylene chloride (CH_2Cl_2), chloroform ($CHCl_3$), 1,2-ethylene chloride, and hydrochloric acid (HCl) were used as received.

2.2. Polymer synthesis

Poly (L-lactide) (PLA) with the molecular weight of 85, 000 g/mol was prepared in our lab by the ring-opening polymerization of LLA. The triblock copolymer PLA-b-AP-b-PLA (PAP) of PLA and aniline pentamer (AP) was synthesized by coupling an electroactive carboxyl-capped AP with two biodegradable bihydroxyl-capped PLAs via a condensation reaction according to our previous paper (Scheme 1) [36]. It was blended with PLA for the following study because of its lower molecular weight (Mw = 12, 410, analyzed with GPC). PANi with the molecular weight of 60,520 (Mw) was synthesized and provided by Prof. Xianhong Wang, Changchun Institute of Applied Chemistry, China.

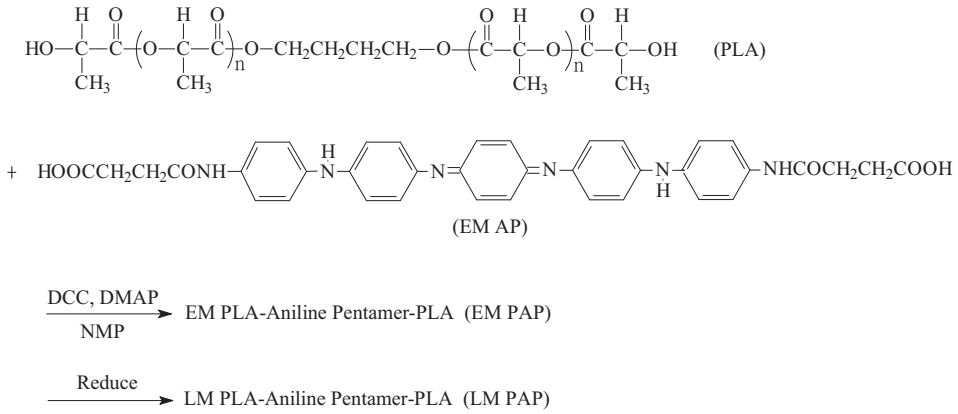

Scheme 1. Synthesis of electroactive PAP triblock copolymer.

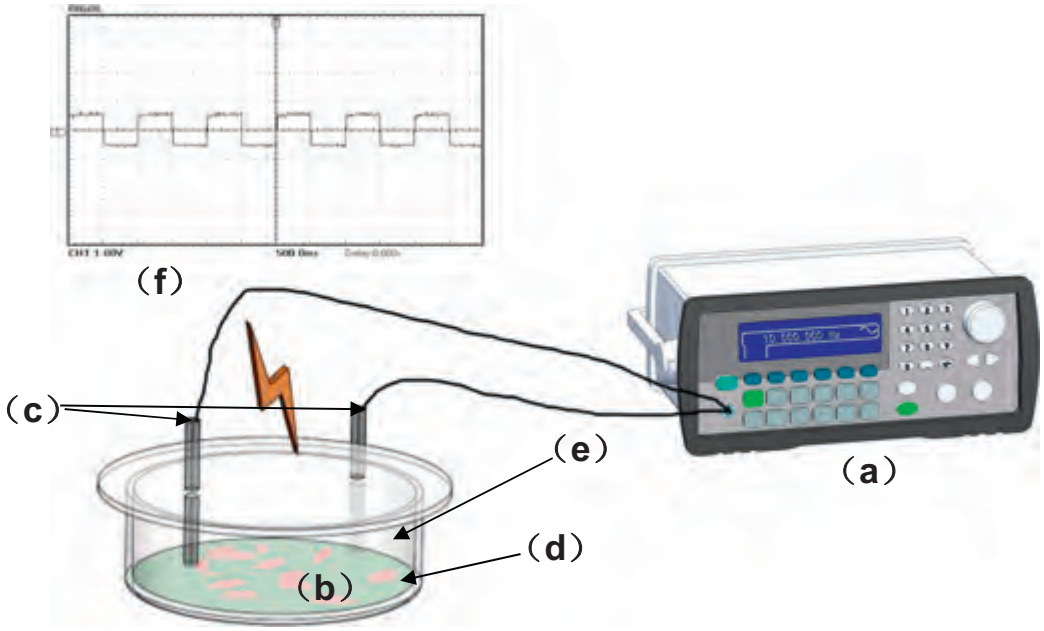

Scheme 2. Schematic cell culture system coupled with electrical stimulation. It consists of a function signal generator (a), a cell culture plate (b), and double platinum (Pt) electrodes (c) and coverslips covered with polymer thin films (d) both immersed in the culture medium (e). The wave form of electrical signals (f) is monitored by a digital oscilloscope.

2.3. Polymer thin film preparation

PAP/PLA (w/w = 1:1) were dissolved respectively in chloroform to form a 1 wt% homogeneous solution. Then camphor-10-sulfonic acid (CSA) was added to the PAP/PLA solution ($W_{CSA}/W_{PAP}/W_{PLA}$ = 0.15:1:1). The solutions were respectively coated onto a glass coverslip of 24 mm × 24 mm (square one) or 15mmin in diameter (round one) to form a layer of thin film. The coverslips were pretreated with 2% dimethyl dichlorosilane (DMDCS, Fluka)/chloroform solution and dried at 180 °C for 4 h. The solvent in the thin films was removed by drying in the air for 30 min and then under vacuum for 48 h at room temperature. The coverslips with the thin films were then sterilized under UV light for 30 min. Similarly, PLA and PANi films were prepared as controls. The glass control was the cleaning coverslips untreated with DMDCS.

2.4. Characterization and measurement

Atomic force microscopy (AFM) experiments were performed by using SPI 3800/SPA300HV (Seiko Instrument Inc.) in tapping mode to observe the surface topography. The microstructure of PAP copolymer was studied by transmission electron microscopy (TEM), using JEOL JEM-1010 electron microscope. Dynamic light scattering (DLS) measurements were carried out with a DAMN EOS instrument equipped with a He–Ne laser at the scattering angle of 108°. The solutions of PAP/PLA about 1 mg/mL were passed through a 0.45 μm filter before the measurements. Water contact angle at the surface of the samples (PLA, PANi and PAP/PLA) were examined by a commercial contact angle system (DataPhysics, OCA 20). 3 points on the surface of each sample were measured, and the average was taken as the water contact angle of the sample.

2.5. Cell culture

H9c2 cell line (H9c2), purchased from Institute of Biochemistry and Cell Biology, Shanghai Institutes for Biological Sciences, Chinese Academy of Sciences, was a subclone of the original clonal cell line derived from embryonic BD1X rat heart tissue and exhibited many of the properties of skeletal muscle [37]. The cells were cultured with Dulbecco's modified Eagle's medium (DMEM, GIBCO) supplemented with 20% FBS (GIBCO), 1.0 × 10^5 U/L penicillin (Sigma), 100 mg/L Streptomycin (Sigma) in a humidified incubator at 37 °C and 5% CO_2. The medium was refreshed every 2 days. After 7 days culture, the monolayer H9c2 cells were removed respectively from the cell culture flasks by trypsin (2.5 mg/ml) and EDTA (0.2 mg/ml) (1:1, v/v) treatment, and rinsed three times with 0.1 M PBS by centrifugation at 1000 rpm for 5 min. The obtained cells were re-suspended in the medium to adjust cell density before use.

2.6. Cell attachment and spreading

Cell attachment and spreading of H9c2 cells on PLA, PANi and PAP/PLA at different time intervals were studied. The coverslips coated with the thin films of PLA, PANi and PAP/PLA were placed into 6-well plates (Costar). The coverslips without polymer coating were used as the control. The wells were washed three times with PBS and added with 3 ml/well of DMEM containing 20% FBS to prevent the coverslips from floating up. A density of 2.0 × 10^4 cells in 1 ml of medium were then seeded into each well, and the plates were incubated at 37 °C and 5% CO_2 for 4 h, 6 h, 24 h or 48 h, respectively. Then the coverslips were washed with PBS for three times and fixed with 2.5% glutaraldehyde at room temperature for 10 min. The cells were dyed with fluorescein isothiocyanate (FITC, SIGMA) for 8 min, and washed with distilled water for 5 times. Cell attachment and morphology were observed under the fluorescent reverse microscope (TE2000U, NIKON). For each specimen, nine pictures were taken by Digital Camera DXM1200F (NIKON).

2.7. Electrical stimulation

A modified cell culture system coupled with electrical stimulation was designed according to our previous work [38]. As shown in Scheme 2, the system consisted of a function signal generator (SUING, TFG6030), a 6-well or 24-well cell culture plate, platinum (Pt) electrodes, and cover-sides covered with polymer thin films. The square wave form of electrical signals was monitored by a digital oscilloscope (Rigol, DS1022C). The double Pt electrodes with the distance slightly less than the wells' diameter were fixed on the covers of cell culture plates and had enough lengths to touch into the medium. The coverslips with the polymer films were placed onto the bottoms of wells and the cells were seeded on the coverslips between the two Pt electrodes. All Pt electrodes were connected with copper conductor cables in the form of

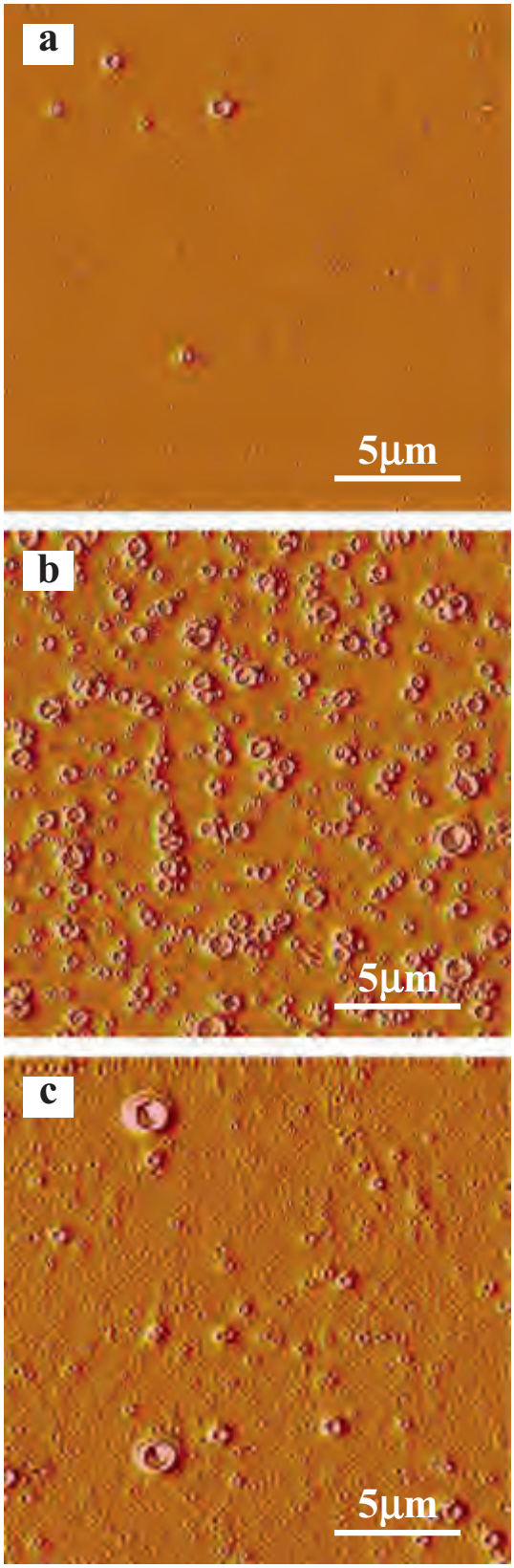

Fig. 1. AFM amplitude images of the film surface topography of PLA (a), PANi (b) and PAP/PLA (c).

parallel circuit. This equipment ensured uniform current fluxes through all the wells. Before electrical stimulation, H9c2 cells were grown for 24 h to allow settling and adhesion. Pulse electrical stimulation of 5 V/1 Hz/500 ms, that is a voltage (or amplitude) of 5 V (± 2.5 V), a frequency of 1 Hz and a pulse duty ratio of 50%, was undertaken for 1 h each day if it was not specifically stated. The medium was refreshed every 2 days. To observe the effects of different electric signals on cell morphology, the parameters of amplitude (3 V and 5 V), frequency (1 Hz, 10 Hz and 20 Hz) and pulse duration (2 ms, 25 ms, 50 ms and 100 ms) were varied.

2.8. Cell proliferation

The proliferation of H9c2 on the surfaces of PLA, PANi, PAP/PLA and the control glass with or without electrical stimulation was determined using the 3-(4,5-dimethylthiazoyl-2-yl)-2,5-diphenyltetrazolium bromide (MTT) assay. Cells at a density of 0.5×10^4 cells/2 ml/well were seeded on the round coverslips (15.5 mm in diameter) coated with different materials in 24-well cell culture plates. The coverslips without polymer coating were used as the control. Two groups were designed for each material, including an unstimulated group and a stimulated group. 4 parallels were set up for each group. After cultured in a humidified incubator containing 5% CO_2 at 37 °C for 24 h to allow settling and adhesion, the cells were given an electrical stimulation for 2 or 5 days. Then 150 μl of MTT solution was added to each well. After incubation at 37 °C for 4 h in a humidified incubator, the medium was discarded and the precipitated formazan was dissolved in 750 μl 0.04 M HCl/isopropanol. The optical density of the solution was evaluated using a microplate spectrophotometer (Thermo Electron MK3) at a wavelength of 540 nm. The mean value of the four readings for each sample was used as the final result.

2.9. Cell morphology

Cell morphological changes of H9c2 on the surface of the different materials treated with electrical stimulation were observed. Briefly, after settling and adhesion of 24 h, H9c2 cells seeded respectively on glass, PLA, PANi and PAP/PLA were given an electrical stimulation for 6 days. The cells were then dyed with FITC stain and the pictures of cell morphology were captured with the fluorescent reverse microscope. The pulse electrical stimulations of 3 V/20 Hz, 5 V/1 Hz and 5 V/20 Hz with a 50% pulse duty ratio were employed. Meanwhile, H9c2 cells on PAP/PLA and glass response to different pulse electric signals of 3 V/1 Hz/100 ms, 3 V/20 Hz/2 ms, 5 V/1 Hz/2 ms, 5 V/1 Hz/50 ms, 5 V/10 Hz/2 ms(e) and 5 V/20 Hz/2 ms were observed.

2.10. Calcium measurement

Cells were seeded on glass or PAP/PLA, and then electrical stimulation was applied for 5 days. The medium was removed and washed three times with KB buffer (70 mM KOH, 40 mM KCl, 20 mM KH2PO4, 3 mM $MgCl_2{\cdot}6H_2O$, 1.5 mM CaCl2, 0.5 mM EDTA, 50 mM L-glutamic acid, 20 mM aminoethylsulfonic acid, 10 mM glucose and 10 mM HEPES, pH 7.4). The cells were then treated with 1 mM Fluo-2 acetoxymethyl ester (fura-2-AM) (emulsified freshly with F127 in KB solution) in 5% CO_2 at 37 °C for 30 min, and placed on the stage of an inverted microscope (TE2000U, NIKON) with a computerized ion imaging system (cool SNAP DG-4, Pholomatrics, U.S.A) allowing rapid filter-change for dual wavelength excitation (340 and 380 nm). Images of calcium signal were obtained, and the ratios of calcium-bound (340 nm) and free (380 nm) Fura-2 were analyzed and calculated automatically in order to determine intracellular free calcium levels [39].

2.11. Statistical analysis

Quantitative data were presented as means ± standard deviation (SD) and statistical analysis was assessed using SPSS (v11.5). Then One-way analysis of variation (ANOVA) was performed on the data, followed by LSD and S-N-K multiple comparison procedures. A value of

$p < 0.05$ was considered to be statistically significant.

3. Results and discussion

3.1. Electrochemical properties and conductivity of PAP

The electrochemical properties and conductivity of PAP had been investigated in our previous work [36]. The results showed that the copolymers possessed good electroactivity and its conductivity (10^{-5}–10^{-6} S/cm) was in the semiconductor region, decreased a lot compared to that of AP and PANi.

3.2. Surface topography

As shown in Fig. 1, the surface topography of PLA, PANi and PAP/PLA thin films were observed with AFM. The amplitude images of AFM showed that PANi and PAP/PLA presented the rough surfaces compared to that of PLA, and the surface of PANi was the most roughness because of the hard solubility of PANi. The relative homogeneous roughness of PAP/PLA might result from the solubility of the PAP copolymer. Although the dissolution of the PAP copolymers in $CHCl_3$ was improved over AP because of the PLA segments, micro-phase separation of AP segments could result in the assembly of PAP triblock copolymer (See Scheme 3).

3.3. The microstructure of PAP copolymer

The above-mentioned results were further verified by TEM observation of the microstructure of PAP copolymer. Fig. 2a show the TEM image of PAP/PLA thin film. The relative homogeneous distribution of black particles of about 150–200 nm in diameter was observed clearly in PAP/PLA, which represented the assembly of the AP segments because of their micro-phase separation in chloroform. The white areas represented the PLA segments and the PLA matrix. DSL analysis showed that the average particle size of PAP copolymer in chloroform solution was 157.2 ± 18.4 nm (see Fig. 2c). Compared with the PAP copolymer, the particles of PANi were larger and more unhomogeneous (Fig. 2b). Although the TEM image of PAP/PLA thin film in present study was greatly different from that of PAP copolymer prepared by ultracryotomy [36], the results of present study approved our previous speculation that the interlaced distribution of the PLA segments and the AP segments is homogeneous. Spontaneous self-assembly in water of the electroactive triblock copolymer of poly (ethylene glycol) (PEG) and aniline pentamer (AP) has also been reported in our previous paper [40]. In the PAP copolymer, PLAs are the soft segments and AP is the hard segment. The regular structure (soft-hard-soft) of triblock copolymer contributes to its special biological properties. First, the PLA chains are bonded on the two ends of the AP to increase its biocompatibility and apparent solubility. Second, the interface surface of the PAP copolymer with homogeneous electroactive areas was formed by spontaneous self-assembly. Thus, the soft PLA segments trend to aggregate together to form a continuous matrix, while the hard ones

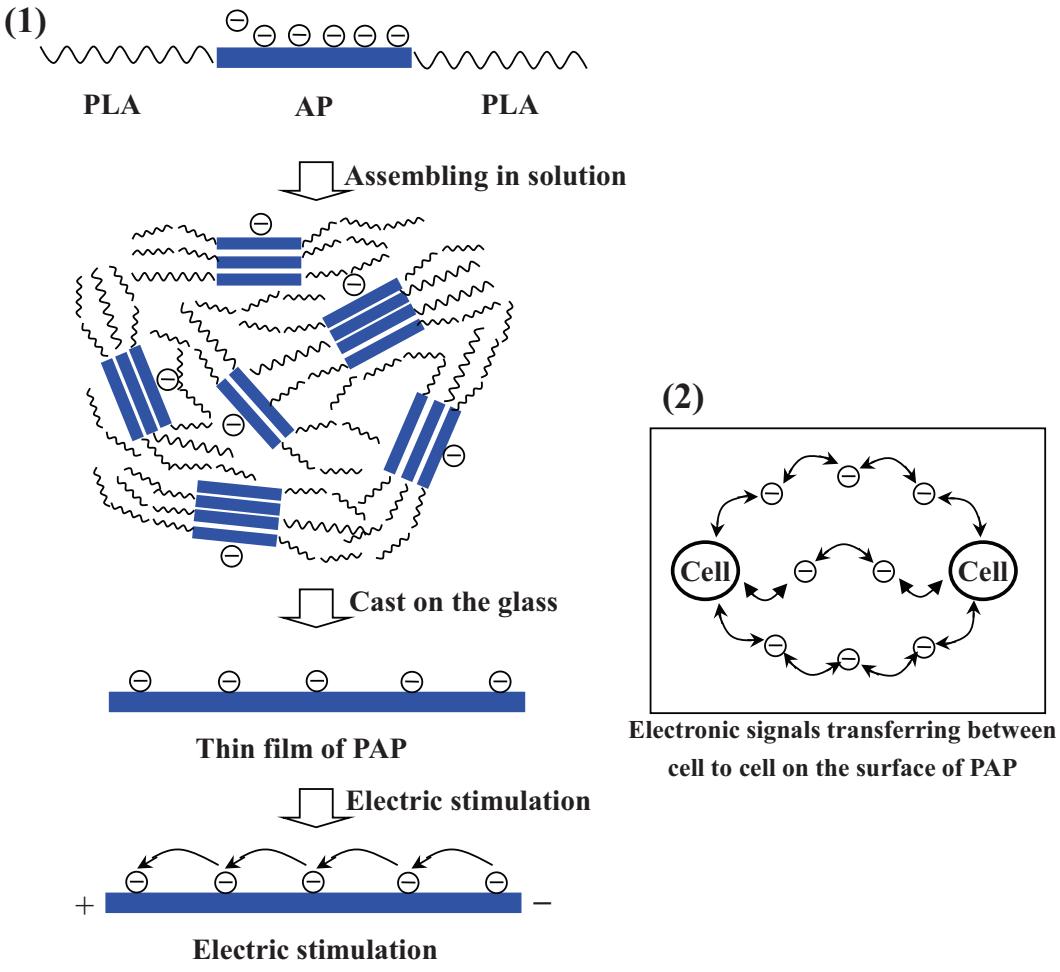

Scheme 3. Schematic illustration of electroactivity and electric conductivity of PAP copolymer (1) and its roles in electronic signals transferring between cell to cell (2).

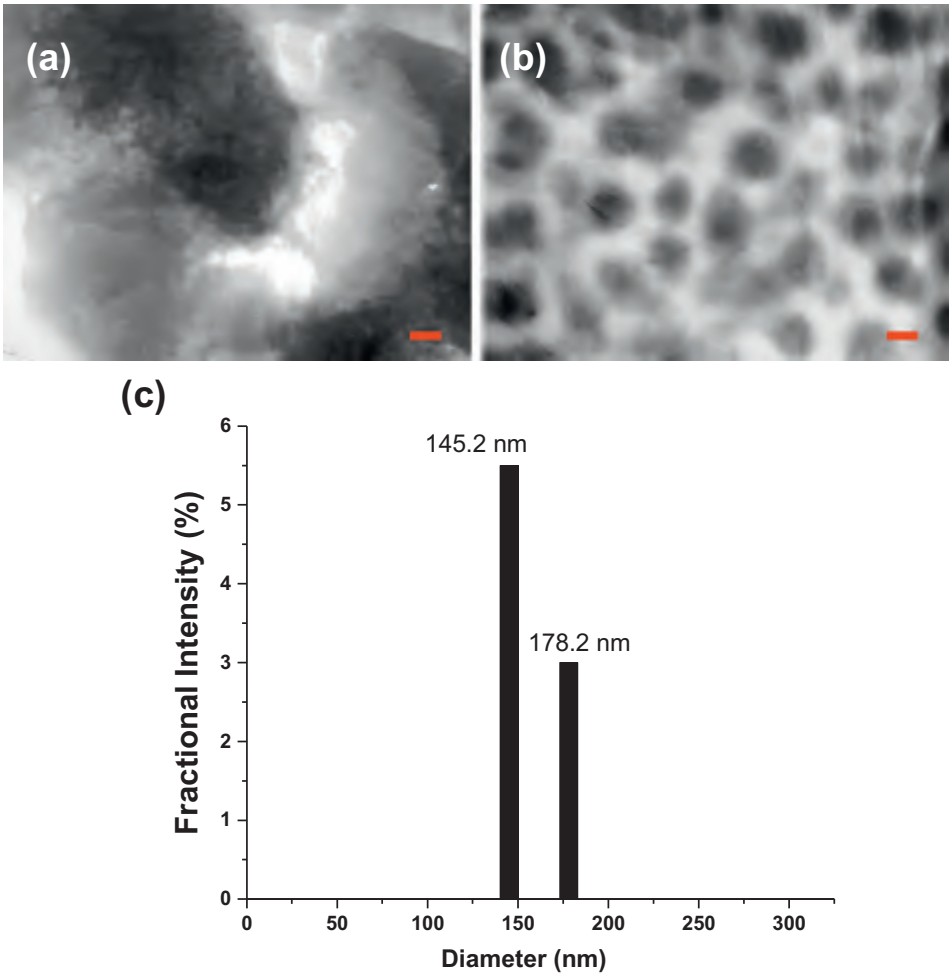

Fig. 2. TEM images of PAP/PLA (a) and PANi (b). Scale bars are 100 nm. (c) Size distribution of the aggregates of PAP copolymer measured by DLS.

may form discontinuous domains. Within an AP domain the electric conduction is easy while between two adjacent domains the electric conduction might be realized through the tunnel effect through the PLA matrix, which could be served as the bridge of cell signals transferring (see Scheme 3).

3.4. Surface hydrophilicity

The surface hydrophilicity of the thin films of PLA, PANi and PAP copolymer, as characterized by static water contact angle, is shown in Fig. 3. The PLA sample presented lower hydrophilicity and its contact angle was 73.3 + 1.1° higher than that of PANi and PAP. The contact angle of PANi was only 40.7 + 1.9°. The hydrophilicity of PAP/PLA was between PLA and PANi and its contact angle is 46.6 + 1.3°. Compared to PLA, the hydrophilicity of PAP/PLA was improved because of introduction of AP segment in PAP copolymer.

3.5. Cell attachment and cell spreading without electric stimulation

It has been well known that cell adhesion is an important cellular process because it directly influences the following proliferation of cell and forming of tissue. In general, cell behavior and interaction with a bioactive material surface are dependent on the properties such as topography, surface charge and chemistry [41]. Fig. 4 shows cell morphology of H9c2 cells attached and grown on glass, PLA, PANi and PAP thin film after seeding for 4 to 48 h. The cells attached and grew better on PAP/PLA than those on PLA, PANi at any time period, which was similar to that on glass.

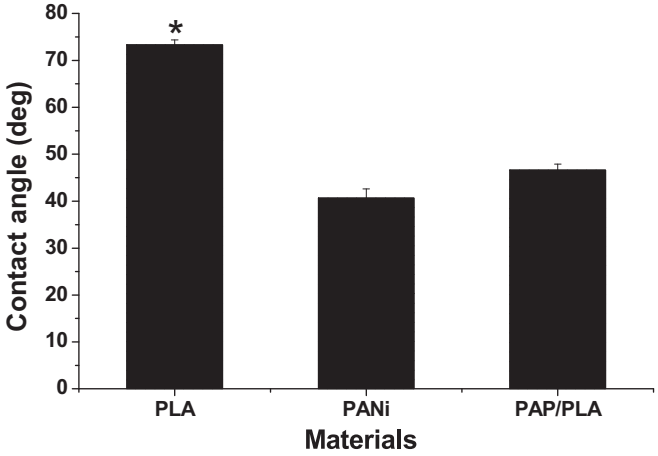

Fig. 3. Water contact angle of the thin films of PLA, PANi and PAP/PLA. * indicates $p < 0.05$ compared to the other groups, n = 3.

3.6. Effects of electrical stimulation on cell proliferation and cell morphology

As shown in Fig. 5, the cell proliferation of H9c2 cells on different materials with or without electrical stimulation was evaluated using MTT test. Compared with the unstimulated group, the numbers of cells on all substrates in stimulated group increased significantly at 3- or 6-day cell culture ($p < 0.05$). At 3-day, the number of cells on PAP/PLA

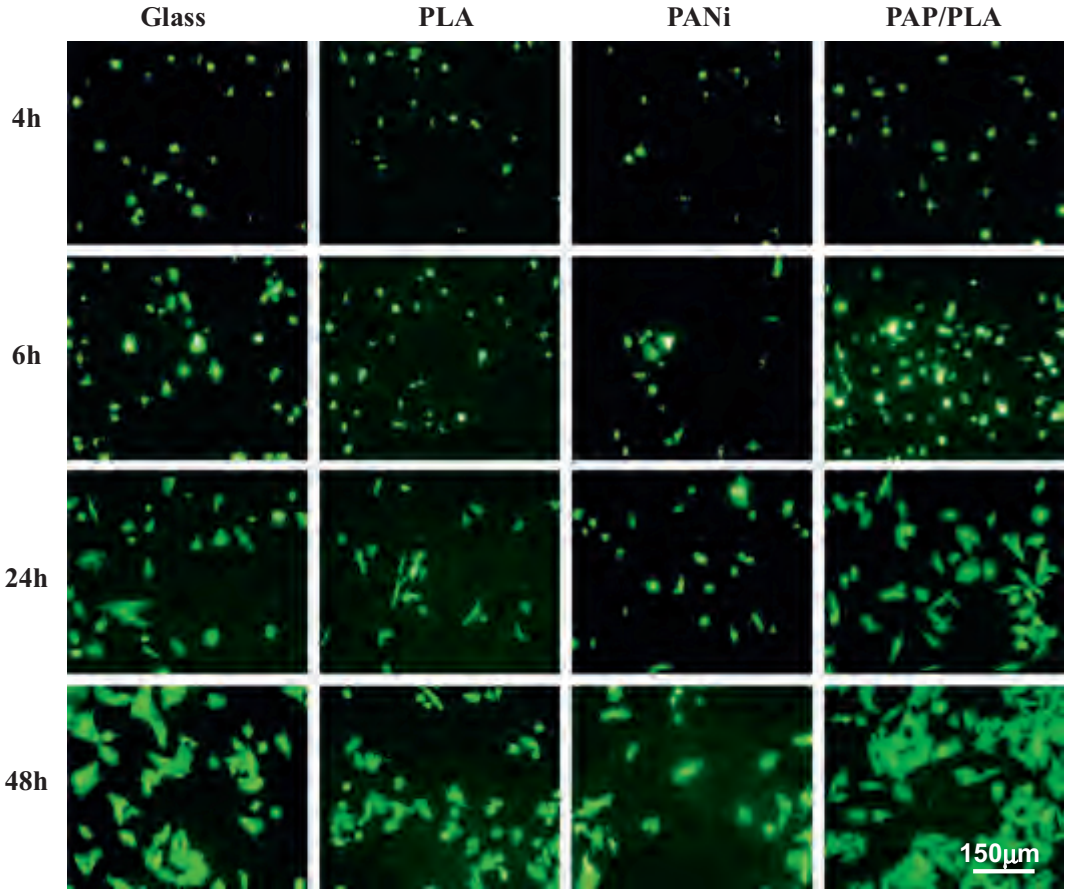

Fig. 4. Fluorescein isothiocyanate (FITC) staining showed that H9c2 attached, spread and grew on glass, PLA, PANi and PAP/PLA for 4–48 h. The electroactive copolymer of PAP improved cellular adhesion, spreading and growth in vitro obviously. The scale bar of all pictures is 150 μm.

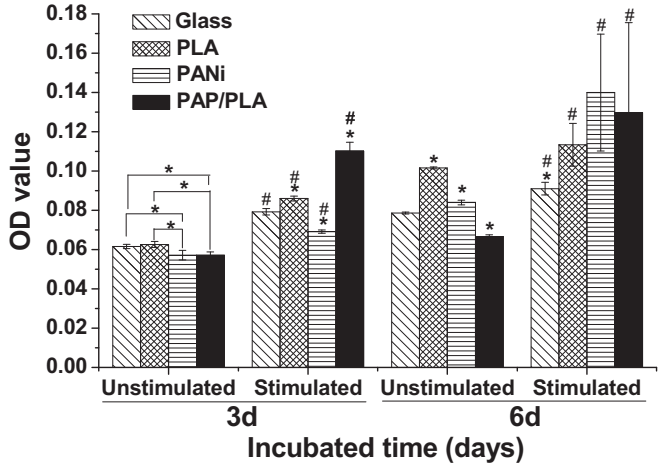

Fig. 5. MTT assay showed the optical values of H9c2 cells on glass, and the thin films of PLA, PANi and PAP/PLA treated with electric stimulation (5 V/1 Hz/500 ms, 1 h/day, started from 24 h after seeding) for 2 and 5 days. * indicates $p < 0.05$ compared to the other groups and # indicates $p < 0.05$ compared to the same materials unstimulated, n = 4.

was the most in stimulated group and had the largest increase (nearly twofold) compared to unstimulated group ($p < 0.05$). There was larger cell number on PLA and smaller cell number on PANi compared to that on glass ($p < 0.05$). At 6-day, the numbers of cells on both PANi and PAP/PLA in stimulated group were slightly higher than that on PLA ($p > 0.05$) and significantly higher than that on glass ($p < 0.05$). They also had larger increases than those on PLA and glass compared to unstimulated group. Our results get well along with those studies on electrical stimulation in literatures. Pedrotty et al. have reported that electrical stimulation could enhance the proliferation of cardiac myocytes on 3-D polyglycolic acid (PGA) mesh scaffolds [42]. At 3-day, PANi had the lowest cell proliferation both in the electrical stimulation group and non-electric stimulation, probably mainly due to the fact that its monomer, aniline, and other reaction byproducts, especially the aniline dimer benzidine that is formed during PANi synthesis [43,44]. At 6-day, after two changes of medium, the cell proliferation of PANi group increased gradually with the decrease of the concentration of monomer, aniline, and other reaction byproducts. In the electrical stimulation condition, the cell proliferation of the PNAi group reached the PAP/PLA group, which was no significant difference. Besides this, the present study elicits that the proliferation of H9c2 cells stimulated electrically could be further promoted by growing on the surface of conductive or electroactive polymers.

The morphological change of H9c2 cells on different substrates (glass, PLA, PANi and PAP/PLA) with or without electrical stimulation is shown in Fig. 6, under the electrical stimulation 1 h a day for 6 days, the cells grown on all substrates sprouted “pseudopodia”. Among them, PAP/PLA (Fig. 7h–j) had the greater number of cells with “pseudopodia” compared with those on PANi, PLA and glass (Fig. 6b, d, f). However, under the absence of electrical stimulation, only a small number of “pseudopodia” were observed in the PAP/PLA and PANi groups, and the length and number of “pseudopodia” were less than that of the electric stimulation group. The “pseudopodia” always grew towards another cell and appeared to arrangement with a certain orientation. As shown in Scheme 3, it might be the need of cells for enhancing their communication, and its formation might be associated with electroactivity of the PAP copolymer and driven by electrical

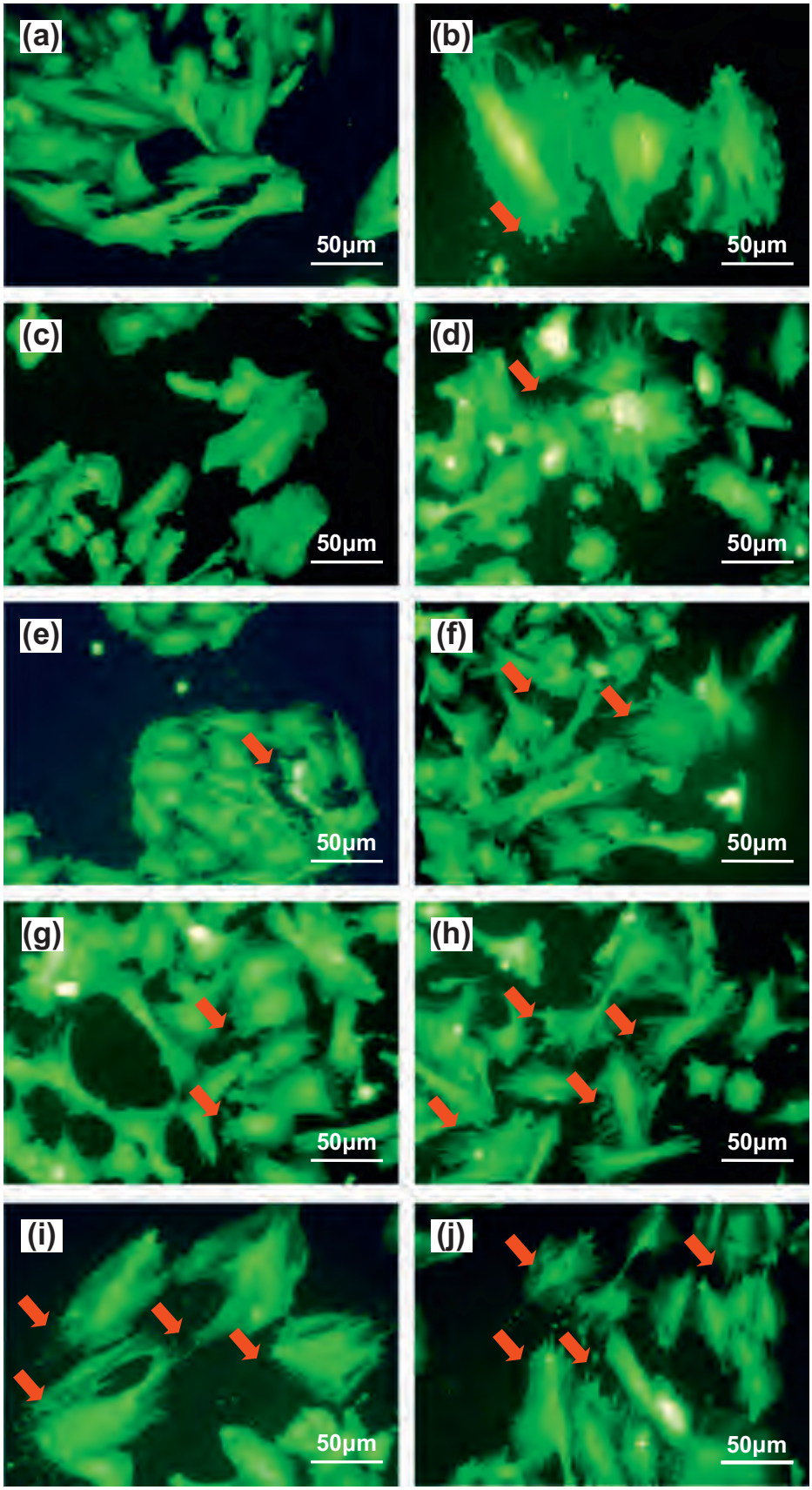

Fig. 6. The "pseudopodia" of H9C2 emerged on the thin films stimulated electrically for 6 days. The cells were growing on glass (a and b), PLA (c and d), PANi (e and f), and PAP/PLA (g–j). (a, c, e and g) were unstimulated; (b, d, f and g) were stimulated with 5 V/1 Hz/500 ms. (i and j) were stimulated with 3 V/20 Hz/25 ms (b) and 5 V/20 Hz/25 ms (d), respectively. The electrical stimulation started from 24 h after cell seeding, and for 1 h per day. All scale bars are 50 μm, the red arrow indicated the "pseudopodia". (For interpretation of the references to color in this figure legend, the reader is referred to the web version of this article.)

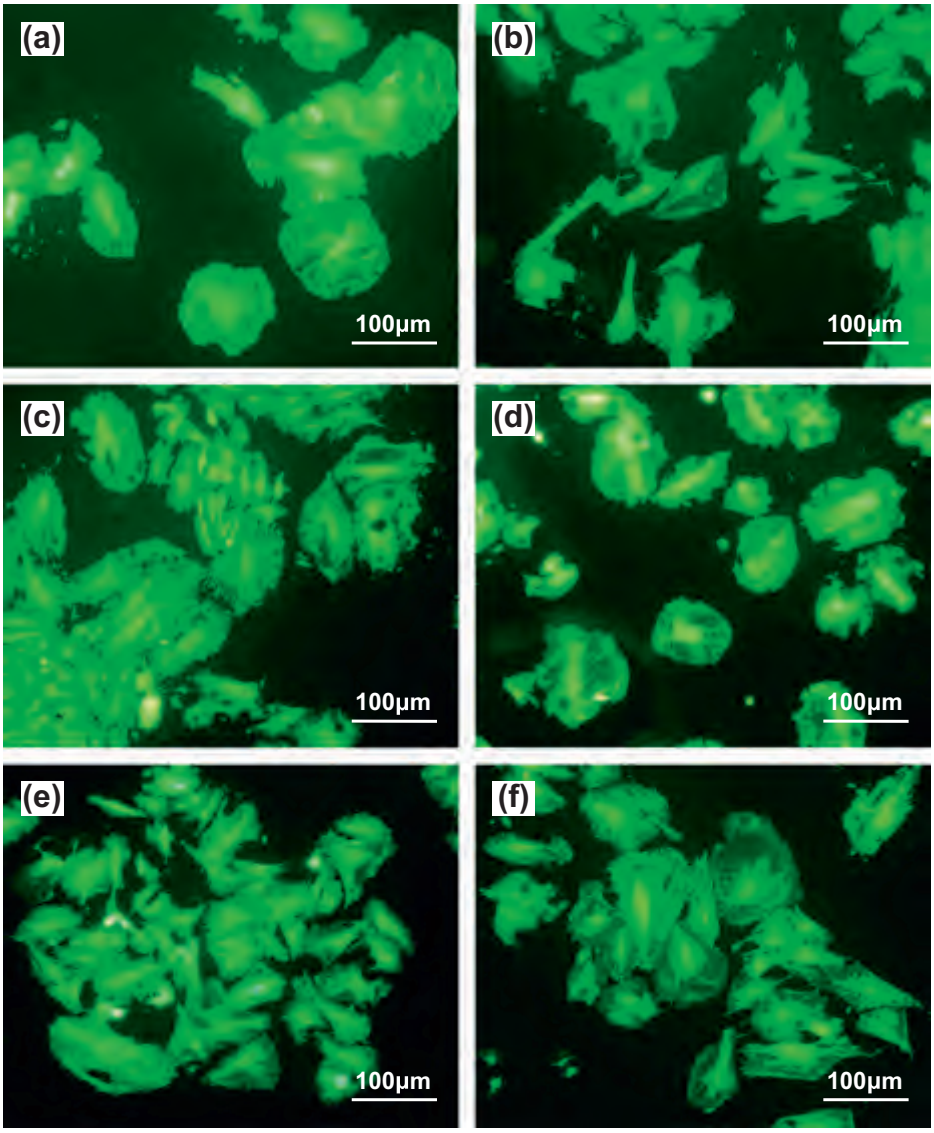

Fig. 7. Representative FITC fluorescent micrographs of H9c2 growing on PAP/PLA for 9 days. The cells were treated with electric stimulation of 3 V/1 Hz/100 ms (a), 3 V/20 Hz/2 ms (b), 5 V/1 Hz/2 ms (c), 5 V/1 Hz/50 ms (d), 5 V/10 Hz/2 ms (e), 5 V/20 Hz/2 ms (f) for 6 days from the second day after cell seeding, 0.5 h/day. Scale bars are 100 μm.

potential. According to the literature, the "pseudopodia" is the possible beginning of formation of myocardium intercalated disk [45]. On a molecular level, electrical stimulation promoted the levels of cardiac proteins and up-regulated the expression of the corresponding genes. Myosin heavy chains were the basic unit of myosin and played an important role in the working myoblasts. The expression of myosin heavy chains was decreased in non- stimulated and increased in stimulated cardiomyocytes, suggesting that the maturation of cardiomyocytes depended both on culture duration and electrical stimulation [46]. Changes in cell morphology had been also found after the effects of pulsed electrical stimulation. HFF-1 human newborn fibroblasts and Balb/3T3 clone A31 mouse embryonic fibroblasts were stimulated by 5 ms pulses with a frequency of 0.5 Hz for 1–72 h. Cell-to-cell interactions via cellular projections were found. Anisodiametric, multinucleated, myotubelike structures with pole-to-pole cell fusion and fiber rearrangements resembling a striated-muscle-like phenotype could be observed as early as 24 h after ES treatment [47]. These results revealed the possible mechanism of morphological changes in cardiac myoblasts under electrical stimulation. In this study, the PAP copolymer itself could improve the electrophysiological interaction between two neighbouring cells by providing a conductive and electroactive surface, but the effect was limited and it could be enhanced by the treatment of electrical stimulation.

3.7. Effects of different electric pulse signals on cell morphology

The cell morphology of H9c2 on PAP copolymer influenced by different electric pulse signals (3 V/1 Hz/100 ms, 3 V/20 Hz/2 ms, 5 V/1 Hz/2 ms, 5 V/1 Hz/50 ms, 5 V/10 Hz/2 ms, 5 V/20 Hz/2 ms) were further observed. As shown in Fig. 7, the shapes of H9c2 cells on PAP/PLA thin film varied on electric pulse signals obviously. At the same levels of frequency and pulse duration (20 h/2 ms), the cells seemed to be enlarged with the increasing of amplitude from 3 V to 5 V (Fig. 7b and f). When the amplitude and pulse duration were kept in the same levels of 5 V/2 ms, the cell shapes changed slightly, but the cell area decreased with the increasing of frequency from 1H or 10H to 20H (Fig. 7c, e and f). Meanwhile, pulse duration seems to be another important factor which greatly influenced on cell shapes. When the pulse duration was prolonged > 50 ms or 100 ms, H9c2 cells were getting larger and more rounder (Fig. 7a and d). In the work of Chen Chuan et al., under 10 V/1 Hz pulsed electric stimulation, the cell morphology of H9C2 became slender, cells presented an ordered arrangement of

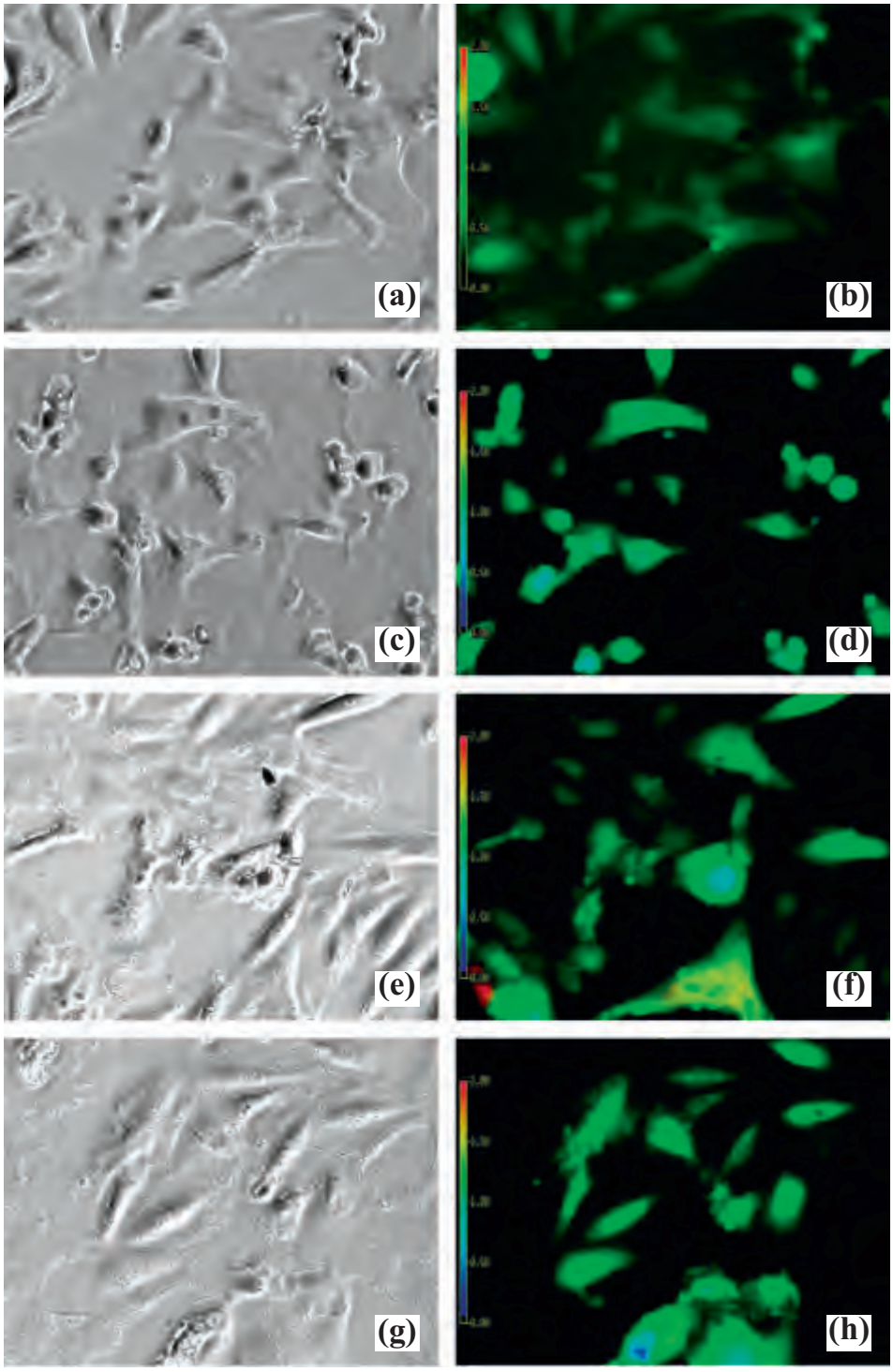

Fig. 8. The effects of electric stimulation (5 V/1 Hz/500 ms) on the concentrations of calcium ions in H9c2 were detected by ion imaging system. (A) The micrographs of H9c2 cells which were seeded and cultured on the surface of PAP/PLA (c, d, g and h) or glass (a, b, e and f) for 6 days, and stimulated electrically (e, f, g and h) for 5 days. a, c, e and g were observed with a light microscope. b, d, f and h were fluorescent micrographs treated with Fura-2-AM. (B) Intracellular calcium concentration of H9c2 cells with or without electric stimulation was analyzed by ion imaging system. (*$p < 0.05$, n = 12).

directions, cell proliferation was decreased, and some cells had pseudopodia structures on the surface. The expression of Oct4 was reduced, while the expressions of cTNT and α-MHC were still strong [48].These results indicated that the relationship between the change of H9C2 morphology and the change of phenotype by differentiation after pulsed electrical stimulation.

3.8. Effects of electrical stimulation on intracellular calcium ions level

Fig. 8 shows the intracellular free calcium concentrations of H9c2 cells on PAP/PLA and glass with or without electrical stimulation measured by a computerized ion imaging system in 6-day cell culture. In each group, 12 cells were selected to determine the intracellular

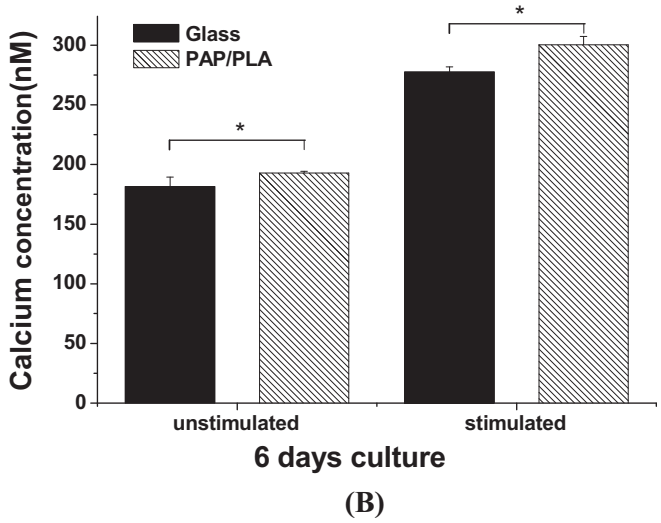

Fig. 8. (*continued*)

calcium ions concentration. Fura-2 is a kind of calcium fluorescence indicator, can be combined with intracellular calcium ions specifically. Excitation wavelength of Fura-2 in calcium-free (380 nm) is longer than in calcium-bound (340 nm). Therefore, the concentration of the calcium ions can be obtained by using the Grynkiewicz formula by detecting the ratio of fluorescence intensity at two excitation wavelengths in calcium-bound and calcium-free [49]. In this study, the free calcium concentration curve was generated directly by ion imaging system.

The calcium ions concentrations of cells on PAP/PLA or glass in stimulated group were higher than those in unstimulated group respectively. In either unstimulated group or stimulated group, the calcium concentrations of cells on PAP/PLA were higher than those on glass. The results showed that the electroactive PAP copolymer may be able to enhance the calcium absorption of cells. According to the literatures, intracellular calcium levels implicated the mechanism for electric field effects on electrical stimulation and educed the proliferation of several other cells types [42]. In cultured sensory neurons, patterned electrical stimulation induced changes in gene expression that was mediated by N- and L-type calcium channels [50]. Moreover, intracellular calcium may play a role in the differentiation of striated myocytes by altering gene expression. In myocytes, except for regulating cellular contraction, calcium plays an important role in intracellular signaling involving cellular differentiation, such as modulating the expression of muscle-specific genes by calcium-signaling pathways and regulating the function of phosphatases and kinases (e.g. calcineurin, CaMK and protein kinase C) that can alter the localization and function of transcriptional activating factors [51]. Thus, we deduced that the PAP electroactive copolymer could accelerate cardiac myoblasts differentiation by improving the level of intracellular calcium assisted with electrical stimulation.

4. Conclusions

A triblock copolymer, PLA-b-AP-b-PLA (PAP), containing one electroactive aniline pentamer (AP) center block and two bilateral biodegradable PLA (PLA) blocks has been synthesized and its potential application in cardiac tissue engineering has been investigated by culture of H9c2 cells. The cell attachment, spreading and proliferation of H9c2 cells was promoted on the surface of the PAP copolymer and enhanced by pulse electrical stimulation. Under the electrical stimulation, the cells on the copolymer emerged the structure of “pseudopodia” and the level of intracellular calcium was increased. Moreover, their morphology could be changed after treatment with the different electrical signals. The behavior and morphological change of cardiac myoblasts may be associated with their differentiation which is deduced by the PAP copolymer. It is regarded that the novel conducting copolymer can enhance electronic signals transferring between cells because of its special electrochemical properties, which may result in the differentiation of cardiac myoblasts.

Acknowledgements

We gratefully acknowledge the financial support from the National Natural Science Foundation of China (No. 51203152, 51473164, 51673186 and 51403197), the Program of Scientific Development of Jilin Province (20170520121JH, 20170520141JH), the joint funded program of Chinese References Academy of Sciences and Japan Society for the Promotion of Science (GJHZ1519), and the special fund for industrialization of science and technology cooperation between Jilin Province and Chinese Academy of Sciences (2017SYHZ0021).

References

[1] K.M. Fischer, C.T. Cottage, W. Wu, S. Din, N.A. Gude, D. Avitabile, et al., Enhancement of myocardial regeneration through genetic engineering of cardiac progenitor cells expressing Pim-1 kinase, Circulation 120 (2009) 2077-U45.
[2] J. Leor, S. Aboulafia-Etzion, A. Dar, L. Shapiro, I.M. Barbash, A. Battler, et al., Bioengineered cardiac grafts - a new approach to repair the infarcted myocardium? Circulation 102 (2000) 56–61.
[3] F. Wang, J. Guan, Cellular cardiomyoplasty and cardiac tissue engineering for myocardial therapy, Adv. Drug Deliv. Rev. 62 (2010) 784–797.
[4] A.M. Gorabi, S.H.A. Tafti, M. Soleimani, Y. Panahi, A. Sahebkar, Cells, scaffolds and their interactions in myocardial tissue regeneration, J. Cell. Biochem. 118 (2017) 2454–2462.
[5] K.L. Christman, R.J. Lee, Biomaterials for the treatment of myocardial infarction, J. Am. Coll. Cardiol. 48 (2006) 907–913.
[6] H.H. Vandenburgh, Bioengineered muscle constructs and tissue-based therapy for cardiac disease, Prog. Pediatr. Cardiol. 21 (2006) 167–171.
[7] W.H. Zimmermann, I. Melnychenko, T. Eschenhagen, Engineered heart tissue for regeneration of diseased hearts, Biomaterials 25 (2004) 1639–1647.
[8] W.H. Zimmermann, K. Schneiderbanger, P. Schubert, M. Didie, F. Munzel, J.F. Heubach, et al., Tissue engineering of a differentiated cardiac muscle construct, Circ. Res. 90 (2002) 223–230.
[9] N.K. Guimard, N. Gomez, C.E. Schmidt, Conducting polymers in biomedical engineering, Prog. Polym. Sci. 32 (2007) 876–921.
[10] H. Peng, L. Zhang, C. Soeller, J. Travas-Sejdic, Conducting polymers for electrochemical DNA sensing, Biomaterials 30 (2009) 2132–2148.
[11] R. Ravichandran, S. Sundarrajan, J.R. Venugopal, S. Mukherjee, S. Ramakrishna, Applications of conducting polymers and their issues in biomedical engineering, J. R. Soc. Interface 7 (2010) S559-S79.
[12] T.J. Rivers, T.W. Hudson, C.E. Schmidt, Synthesis of a novel, biodegradable electrically conducting polymer for biomedical applications, Adv. Funct. Mater. 12 (2002) 33–37.
[13] L. Xia, Z. Wei, M. Wan, Conducting polymer nanostructures and their application in biosensors, J. Colloid Interface Sci. 341 (2010) 1–11.
[14] E.B. Aydin, M. Aydin, M.K. Sezginturk, A highly sensitive immunosensor based on ITO thin films covered by a new semi-conductive conjugated polymer for the determination of TNF alpha in human saliva and serum samples, Biosens. Bioelectron. 97 (2017) 169–176.
[15] L. Fang, B. Liang, G. Yang, Y. Hu, Q. Zhu, X. Ye, A needle-type glucose biosensor based on PANI nanofibers and PU/E-PU membrane for long-term invasive continuous monitoring, Biosens. Bioelectron. 97 (2017) 196–202.
[16] R.A. Green, N.H. Lovell, L.A. Poole-Warren, Impact of co-incorporating laminin peptide dopants and neurotrophic growth factors on conducting polymer properties, Acta Biomater. 6 (2010) 63–71.
[17] B. Alshammary, F.C. Walsh, P. Herrasti, C.P. de Leon, Electrodeposited conductive polymers for controlled drug release: polypyrrole, J. Solid State Electrochem. 20 (2016) 839–859.
[18] M.Y. Li, Y. Guo, Y. Wei, A.G. MacDiarmid, P.I. Lelkes, Electrospinning polyaniline-contained gelatin nanofibers for tissue engineering applications, Biomaterials 27 (2006) 2705–2715.
[19] Q. Zhang, Y. Yan, S. Li, T. Feng, The synthesis and characterization of a novel biodegradable and electroactive polyphosphazene for nerve regeneration, Mater. Sci. Eng. C Mater. Biol. Appl. 30 (2010) 160–166.
[20] G. Kaur, R. Adhikari, P. Cass, M. Bown, P. Gunatillake, Electrically conductive polymers and composites for biomedical applications, RSC Adv. 5 (2015) 37553–37567.
[21] R.T. Richardson, B. Thompson, S. Moulton, C. Newbold, M.G. Lum, A. Cameron, et al., The effect of polypyrrole with incorporated neurotrophin-3 on the promotion of neurite outgrowth from auditory neurons, Biomaterials 28 (2007) 513–523.
[22] X.D. Wang, X.S. Gu, C.W. Yuan, S.J. Chen, P.Y. Zhang, T.Y. Zhang, et al., Evaluation of biocompatibility of polypyrrole in vitro and in vivo, J. Biomed. Mater. Res. A 68A (2004) 411–422.
[23] R.L. Williams, P.J. Doherty, A preliminary assessment of poly(pyrrole) in nerve

guide studies, J. Mater. Sci. Mater. Med. 5 (1994) 429–433.
[24] S. Kamalesh, P.C. Tan, J.J. Wang, T. Lee, E.T. Kang, C.H. Wang, Biocompatibility of electroactive polymers in tissues, J. Biomed. Mater. Res. 52 (2000) 467–478.
[25] H.-S. Kim, H.L. Hobbs, L. Wang, M.J. Rutten, C.C. Wamser, Biocompatible composites of polyaniline nanofibers and collagen, Synth. Met. 159 (2009) 1313–1318.
[26] J.P. Saikia, S. Banerjee, B.K. Konwar, A. Kumar, Biocompatible novel starch/polyaniline composites: characterization, anti-cytotoxicity and antioxidant activity, Colloids Surf. B Biointerfaces. 81 (2010) 158–164.
[27] P. Marcasuzaa, S. Reynaud, F. Ehrenfeld, A. Khoukh, J. Desbrieres, Chitosan-graft-polyaniline-based hydrogels: elaboration and properties, Biomacromolecules 11 (2010) 1684–1691.
[28] A.T. Ramaprasad, V. Rao, G. Sanjeev, S.P. Ramanani, S. Sabharwal, Grafting of polyaniline onto the radiation crosslinked chitosan, Synth. Met. 159 (2009) 1983–1990.
[29] S.I. Jeong, I.D. Jun, M.J. Choi, Y.C. Nho, Y.M. Lee, H. Shin, Development of electroactive and elastic nanofibers that contain polyaniline and poly(L-lactide-*co*-epsilon-caprolactone) for the control of cell adhesion, Macromol. Biosci. 8 (2008) 627–637.
[30] K.D. McKeon, A. Lewis, J.W. Freeman, Electrospun poly(D,L-lactide) and polyaniline scaffold characterization, J. Appl. Polym. Sci. 115 (2010) 1566–1572.
[31] P.H.S. Picciani, E.S. Medeiros, Z. Pan, W.J. Orts, L.H.C. Mattoso, B.G. Soares, Development of conducting polyaniline/poly(lactic acid) nanofibers by electrospinning, J. Appl. Polym. Sci. 112 (2009) 744–753.
[32] P.R. Bidez, S.X. Li, A.G. MacDiarmid, E.C. Venancio, Y. Wei, P.I. Lelkes, Polyaniline, an electroactive polymer, supports adhesion and proliferation of cardiac myoblasts, J. Biomater. Sci. Polym. Ed. 17 (2006) 199–212.
[33] P.M. Crapo, Y. Wang, Small intestinal submucosa gel as a potential scaffolding material for cardiac tissue engineering, Acta Biomater. 6 (6) (2010) 2091.
[34] Y. Haraguchi, T. Shimizu, M. Yamato, A. Kikuchi, T. Okano, Electrical coupling of cardiomyocyte sheets occurs rapidly via functional gap junction formation, Biomaterials 27 (2006) 4765–4774.
[35] O. Abilez, P. Benharash, E. Miyamoto, A. Gale, C.P. Xu, C.K. Zarins, P19 progenitor cells progress to organized contracting myocytes after chemical and electrical stimulation: implications for vascular tissue engineering, J. Endovasc. Ther. 13 (2006) 377–388.
[36] L. Huang, J. Hu, L. Lang, X. Wang, P. Zhang, X. Jing, et al., Synthesis and characterization of electroactive and biodegradable ABA block copolymer of polylactide and aniline pentamer, Biomaterials 28 (2007) 1741–1751.
[37] C. Ding, Y. Wang, S. Zhang, Synthesis and characterization of degradable electrically conducting copolymer of aniline pentamer and polyglycolide, Eur. Polym. J. 43 (2007) 4244–4252.
[38] Y. Wang, H. Cui, Z. Wu, N. Wu, Z. Wang, X. Chen, et al., Modulation of osteogenesis in MC3T3-E1 cells by different frequency electrical stimulation, PLoS One 11 (2016).
[39] K. Sato, T. Adachi, D. Ueda, M. Hojo, Y. Tomita, Measurement of local strain on cell membrane at initiation point of calcium signaling response to applied mechanical stimulus in osteoblastic cells, J. Biomech. 40 (2007) 1246–1255.
[40] L. Huang, J. Hu, L. Lang, X. Chen, Y. Wei, X. Jing, Synthesis of a novel electroactive ABA triblock copolymer and its spontaneous self-assembly in water, Macromol. Rapid Commun. 28 (2007) 1559–1566.
[41] C. Heinemann, S. Heinemann, A. Bernhardt, H. Worch, T. Hanke, Novel textile chitosan scaffolds promote spreading, proliferation, and differentiation of osteoblasts, Biomacromolecules 9 (2008) 2913–2920.
[42] D.M. Pedrotty, J. Koh, B.H. Davis, D.A. Taylor, P. Wolf, L.E. Niklason, Engineering skeletal myoblasts: roles of three-dimensional culture and electrical stimulation, Am. J. Phys. Heart Circ. Phys. 288 (2005) H1620-H6.
[43] J.S. Bus, J.A. Popp, Perspectives on the mechanism of action of the splenic toxicity of aniline and structurally-related compounds, Food Chem. Toxicol. 25 (1987) 619–626.
[44] J.H. Harrison, D.J. Jollow, Role of aniline metabolites in aniline-induced hemolytic-anemia, J. Pharmacol. Exp. Ther. 238 (1986) 1045–1054.
[45] M. Radisic, H. Park, H. Shing, T. Consi, F.J. Schoen, R. Langer, et al., Functional assembly of engineered myocardium by electrical stimulation of cardiac myocytes cultured on scaffolds, Proc. Natl. Acad. Sci. U. S. A. 101 (2004) 18129–18134.
[46] M. Radisic, H. Park, S. Gerecht, C. Cannizzaro, R. Langer, G. Vunjak-Novakovic, Biomimetic approach to cardiac tissue engineering, Philos. Trans. R. Soc. B Biol. Sci. 362 (2007) 1357–1368.
[47] J.A. Genovese, C. Spadaccio, J. Langer, J. Habe, J. Jackson, A.N. Patel, Electrostimulation induces cardiomyocyte predifferentiation of fibroblasts, Biochem. Biophys. Res. Commun. 370 (2008) 450–455.
[48] C. Chen, X. Zhang, Y. Dai, X. Zhang, Effect of pulsed electrical stimulation on the proliferation and differentiation of H9c2 cells, Xi bao yu fen zi mian yi xue za zhi Chin. J. Cell. Mol. Immunol. 29 (2013) 337–340.
[49] G. Grynkiewicz, M. Poenie, R.Y. Tsien, A new generation of Ca^{2+} indicators with greatly improved fluorescence properties, J. Biol. Chem. 260 (1985) 3440–3450.
[50] T.A. Brosenitsch, D.M. Katz, Physiological patterns of electrical stimulation can induce neuronal gene expression by activating N-type calcium channels, J. Neurosci. 21 (2001) 2571–2579.
[51] G.A. Porter, R.F. Makuck, S.A. Rivkees, Reduction in intracellular calcium levels inhibits myoblast differentiation, J. Biol. Chem. 277 (2002) 28942–28947.